

BEHAVIOUR OF TRAPEZOIDAL SHEAR PANELS IN STEEL JOINTS

Eduardo Bayo¹; Alfonso Loureiro²; Manuel Lopez²; Beatriz Gil¹

¹ *Department of Structural Analysis and Design, University of Navarra, Spain*
ebayo@unav.es; bgilr@unav.es

² *Escuela Politecnica Superior, University of Coruña, Spain*
lourerio@cdf.udc.es; manuellopez@cdf.udc.es

ABSTRACT

Previous research has stressed the need for a correct definition of the column panel zone deformations under static conditions due to its influence on the overall sway behaviour of the frame. An increase in frame drift due to panel zone shear deformation may render the frame unserviceable. This may even happen for commonly considered rigid joints. Modelling of the panel is also important for the avoidance of local failure of the columns under ultimate limit state conditions.

The shear behaviour of rectangular column shear panels has been investigated thoroughly and different formula has been proposed to characterize their strength and resistance. Modern codes including Eurocode 3 (EN 1993-1-8, 2005) have included these research advances so that they may be used in common practice. However the case of trapezoidal column panels, formed by beams of different depths at each side of the column, has not been researched as much. Steel connections with beams of unequal size are not currently included in design codes.

This paper deals with the experimental results obtained of the shear behaviour of trapezoidal panels arising from steel joints using commercial sections. Also finite element modelling is carried out to compare results. Current modelling procedures are tested and the results compared with those coming from the experiments and numerical simulation.

1. INTRODUCTION

The characterization of steel joint behaviour and properties have been a matter of research for a number of years, and all the accumulated knowledge has been compiled to a large extent in currently available steel design codes.

One important aspect is the behaviour of the column panel subjected to the shear forces arising from the moments of the adjacent beams as well as the shear forces acting on the columns. Krawinkler et al (1975) reported the importance that panel shear deformations have on the frame behaviour under lateral loads, and proposed a formulation for the stiffness and resistance of shear panels of beam to column connections with beams of equal depths. An alternative formulation has been proposed in the Eurocode 3, part 1.8 (2005). These and other proposed methods allow introducing the flexibility of the joints in both the elastic and inelastic range in order to assess the frame response.

The lines connecting the flanges of beams of unequal depths define a trapezoid within the panel column zone. Hoogenbroom and Blaauwendraad (2000) and

Curtis and Greiner (1996) have proposed analytical and computational methods to characterize the shear behaviour of isolated quadrilateral panels. Recently, Hashemi and Jazany (2012) have investigated the connection detailing of joints of unequal beam depths under seismic loads. One of their conclusions is that inclined stiffeners connecting the lower flanges of the beams perform better than the horizontal ones. Jordao (2008) studied the performance of this type of joints for high strength steel without the use of web stiffeners. As a consequence the stress field at the panel zone becomes rather complex due to the fact that the compression, tension and shear zones are all coupled together. The common failure mode of the experiments carried out was web buckling due to compression. Within the context of Eurocode 3, Jordao et al (2008) also proposed modelling and design recommendations based on modified transformation parameters. A suitable modelling of the joint for global analysis can be achieved by considering the cruciform element proposed by Bayo et al (2006, 2012).

Work remains to be done to better characterize the complex behaviour of steel joints with beams of unequal depths and trapezoidal panels. The study involves a wide large number of variables and intervening factors. Hopefully, future work and results will make it possible to include the design of this kind of joints in design codes. In this paper we present some experimental work and numerical (finite element) results in the hope that they will provide some additional insight into this broad and interesting problem.

The moment rotation diagrams depend on a large number of material, geometrical and loading variables. In this work we concentrate on the shear stiffness and resistance of the trapezoidal panel zone and the additional contribution provided by the elements surrounding the panel such as the column flanges and the beam adjacent to the joint. These elements play a major role in the joint post-elastic reserve shear strength and stiffness. Consequently, stiffeners are included to avoid the effects of other components such as the column web in tension and compression, and the column flange in bending and to prevent as much as possible their interaction with the shear component. For the same reason, only fully welded connections are considered in this investigation. The moments acting at both sides of the joint are the most important contribution to the panel shear force, and they are usually considered as the load variables characterizing the strength and stiffness of the joint. However, the beneficial effect of the column shear should also be considered (particularly in the case of short columns) in the joint stiffness and strength as proposed by Krawinkler et al (1975). The deformation is defined in terms of the average shear distortion of the panel zone (PZ), and it is measured in this investigation by means of two inclinometers located on the middle section of the panel. The aim is to understand the mechanisms of deformation and characterize the moment rotation curves due to the panel shear for this type of joints.

2. EXPERIMENTAL WORK AND FINITE ELEMENT MODELS

The experimental work has been carried out in two different experiments with beams of unequal beam depths. The overall scheme is illustrated in Figure 1. The column is pinned at both ends and actuation is applied at points A and B. Those two points are placed exactly 1 meter away from the column flanges. The beam and column sizes are shown in Table 1. A picture of the experimental set up is depicted in Figure 2.

Table 1. Experimental beam and column configurations.

Test	Column	Deep Beam	Shallow Beam	Depth Ratio	Loading Point	Type of Loading
E1A	HEA 240	HEB 300	HEB 160	1.88	A	Elastic
E1B	HEA 240	HEB 300	HEB 160	1.88	B	Failure
E2A	HEA 240	HEB 300	HEB 180	1.67	A	Elastic
E2B	HEA 240	HEB 300	HEB 180	1.67	B	Failure

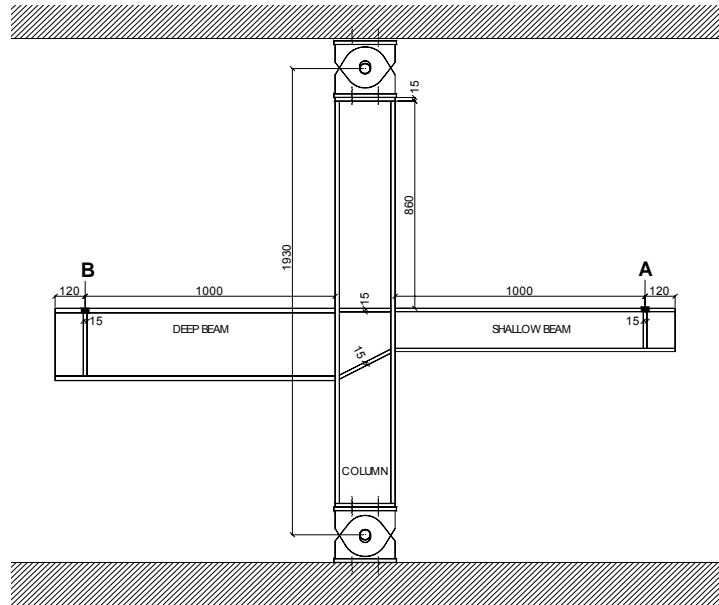


Figure 1. Experimental setup.



Figure 2. Experiment E1 during the loading process.

The top horizontal and the inclined stiffeners were welded as depicted in Figures 1 and 2 to avoid, as mentioned above, any type of failure other than that produced by shear. The stiffeners were 15 mm thick and in all cases were rigid enough to provide the necessary resistance to prevent either tension or compression failure of the column webs, as well as out of plane bending of the column flanges. The type of steel used for all the parts was S275. Coupons were extracted from both the columns and stiffeners to obtain the true properties of the material. Table 2 shows those properties that were subsequently used in the finite element analyses.

The panel was instrumented with 4 strain gages placed at the corners of the panel as shown in Figure 3. They served to monitor the yielding sequence and the levels of shear distortion. Five inclinometers were used as shown in Figure 3 to obtain the rotations. Two were placed vertically at the beams adjacent to the joint. Two more were placed vertically at the top and bottom of the web panel to capture the possible different rotations at those levels. A fifth one was placed in the middle of the panel to capture the rotation of the column due to bending. This rotation is subtracted from those at the beams to obtain the rotation due to the shear deformations.

Table 2. Steel properties obtained from coupons.

Part	σ_y (MPa)	σ_u (MPa)	E (MPa)
HEA 240	330	493	207000
HEA 240	328	494	211000
HEA 240	326	496	209000
HEA 240	329	490	210000
Stiffeners	300	446	213000
Stiffeners	309	449	211000

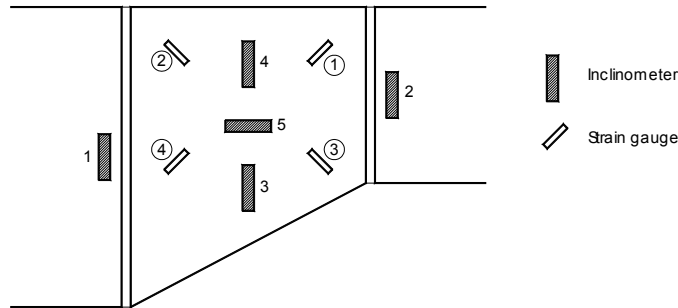


Figure 3. Placement of strain gauges and inclinometers.

The finite element analysis was performed using Abacus®. Solid elements with reduced integration (to avoid shear locking) and hourglass control (C3D8R) were adopted. Figure 4 illustrates part of the model. The material behaviour was introduced by means of the true stress-strain data obtained from the coupons. Static nonlinear material and geometric analyses with force control were performed. The Von Mises yield criterion was selected to define the inelastic response.

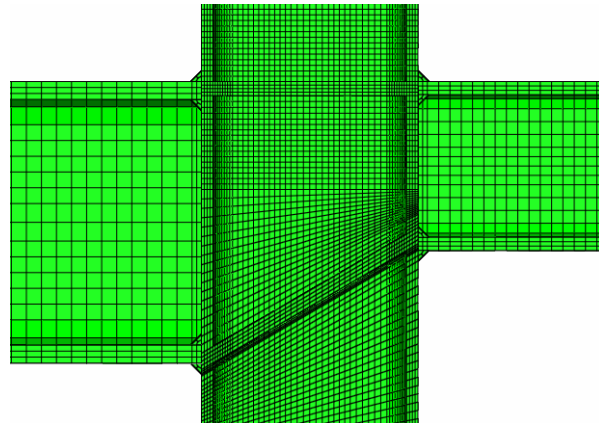


Figure 4. Detail of the finite element model.

3. DESCRIPTION OF RESULTS

The first test E1A consisted in loading the experiment E1 at the tip of the shallow beam (point A). The aim was to obtain the elastic stiffness of the trapezoidal panel under the shear coming from loading the shallow beam. The maximum load applied was 30 kN, and afterwards it was unloaded. A previous finite element analysis had predicted pure elastic behaviour up to that loading level. The shear stress distribution within the panel obtained from the finite element analysis is illustrated in Figure 5a, which corresponds to the level of strains given by the strain gauges shown in Figure 5b.

It may be seen that the stress distribution is very uniform over the upper rectangular part of the panel. The readings of the inclinometers 3 and 4 were similar, and the inclinometers 1 and 2 showed that the rotation at the shallow beam was approximately double the size of the rotation of the deep beam.

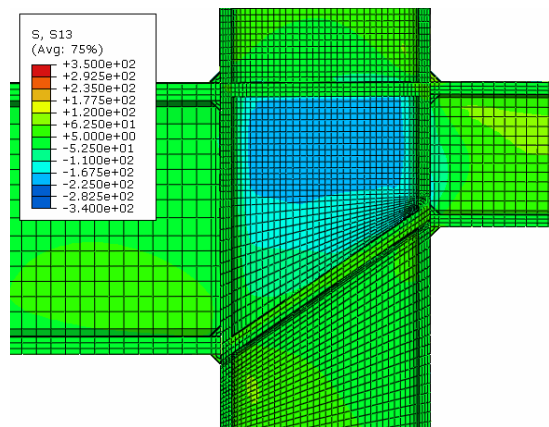


Figure 5a. Shear stress contours in E1A.

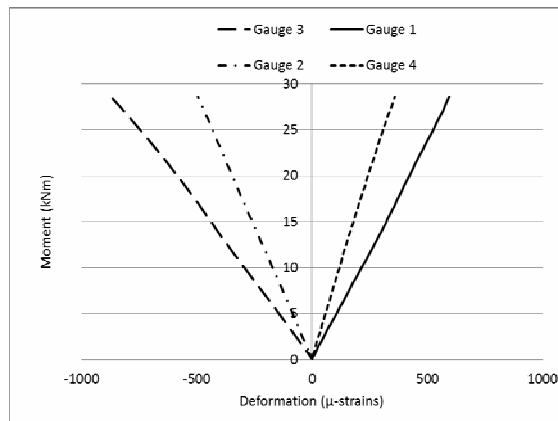


Figure 5b. Strains gauges in E1

The following test, E1B, consisted in loading the experiment E1 at the tip of the deep beam (point B) until failure, which occurred at a load of 230 kN. The shear stress distributions within the panel coming from the finite element analysis during the elastic and inelastic parts of the response are illustrated in Figure 6a and 6b respectively. It may be seen how even in the elastic range the shear stress field now extends more towards the bottom of the panel becoming more trapezoidal in shape.

The readings of the inclinometers 3 and 4 were similar in the elastic range and departed from each other as the inelastic response progressed. The rotation of the lower part of the panel became 35% higher than that of the higher part right before failure. The failure was produced by the cracking of the panel at the upper right corner (right next to strain gauge 1). The angles at the shallow beam were similar to those of the deep beam during the elastic part of the response. However, within the inelastic response the angles at the shallow beam became much larger than those of the deep beam reaching almost 40% more right before failure.

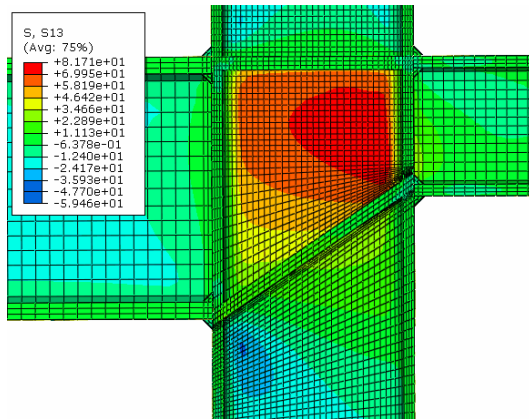


Figure 6a. Elastic shear stress levels in E1B

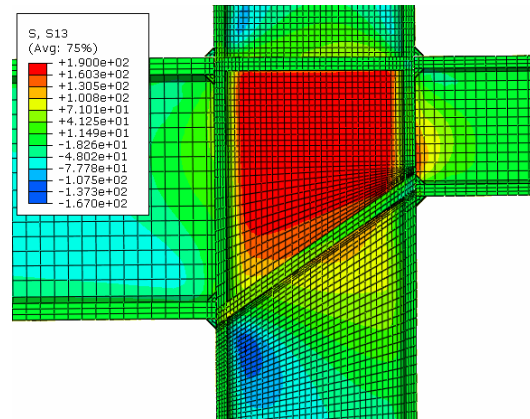


Figure 6b. Plastic shear stress levels in E1B.

The test, E2A, consisted in loading the experiment E2 at the tip of the shallow beam. The qualitative behaviour of this test was similar to that of E1A. The maximum load applied was 37 kN, and afterwards it was unloaded. Again, a previous finite element analysis had predicted pure elastic behaviour up to that loading level. The shear stress distribution within the panel obtained from the finite element analysis is illustrated in Figure 7a, which corresponds with the level of strains given by the strain gauges and shown in Figure 7b. The readings of the inclinometers 3 and 4 were similar, and the rotation at the shallow beam was approximately 60% higher than the rotation of the deep beam.

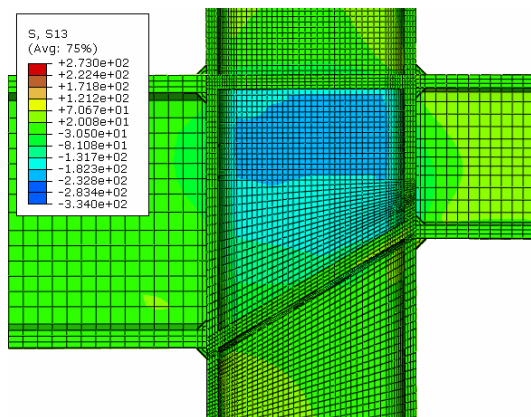


Figure 7a. Shear stress levels in E2A

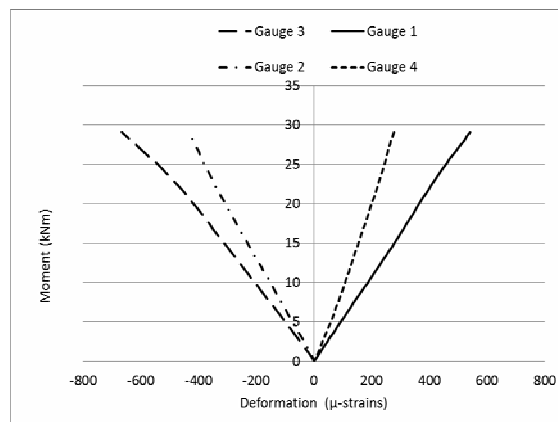


Figure 7b. Strains at gauges in E2A

The final test, E2B, consisted in loading the experiment E2 at the tip of the deep beam (point B) until failure, which occurred at a load of 265 kN. The shear stress distributions within the panel coming from the finite element analysis during the elastic and inelastic parts of the response are illustrated in Figures 8a and 8b respectively. The readings of the inclinometers 3 and 4 were similar in the elastic range and departed from each other as the inelastic response progressed. The rotation of the lower part of the panel became 20% higher than that of the higher part right before failure. The angles at the shallow beam were similar to those of the deep beam during the elastic part of the response. However, within the inelastic response the angles at the shallow beam became much larger than those of the deep beam reaching a difference of 40% right before failure.

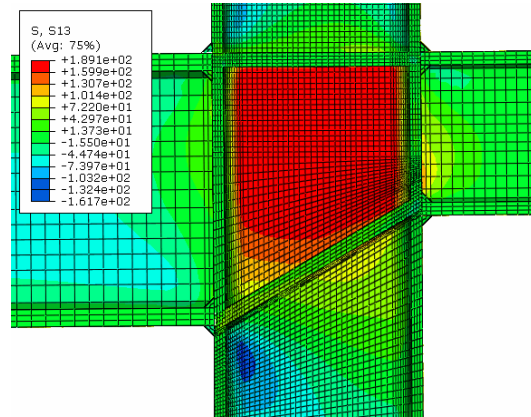
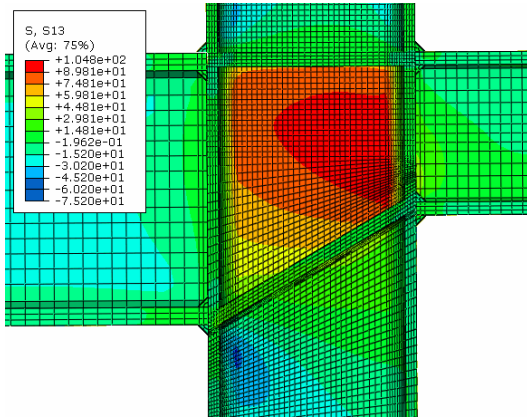


Figure 8a. Elastic shear stress levels in E2B Figure 8b. Plastic shear stress levels in E2B.

The deformed panel and deformed shape of the experiment before failure are shown in Figures Figure 9a and 9b, respectively.



Figure 9a. Panel inelastic deformation



Figure 9b. Deformed shape before failure.

The plastic shear stress levels of the column panel as well as the final deformed shape of the specimen can be seen in Figure 10. It is worth noting how the shallow beam gets much more inclined that the deep beam due to the deformation of the trapezoidal panel as an articulated quadrilateral mechanism.

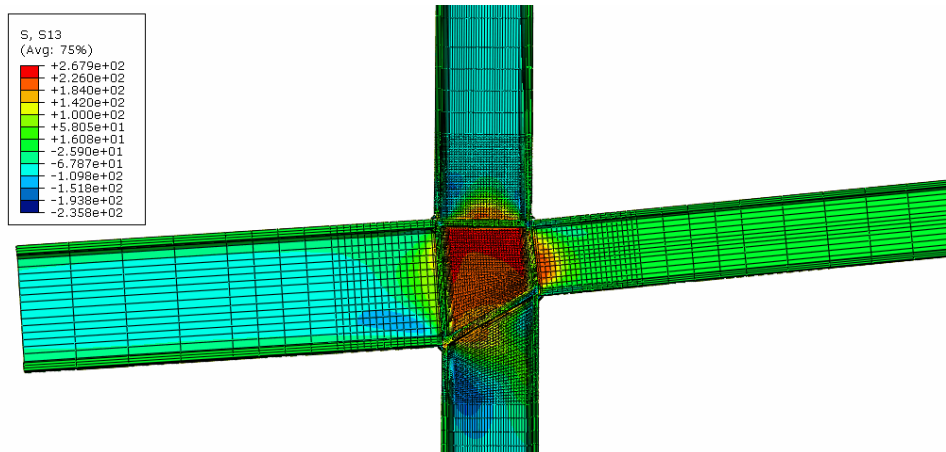


Figure 10. Final stage of stress and deformation in test E2B.

4. MOMENT ROTATION CURVES: STIFFNESS AND RESISTANCE

We compare in this section the moment rotation curves obtained from the experiments, the finite element analysis, the Eurocode 3 and the method proposed by Krawinkler et al (1975). Since the last two do not include trapezoidal panels they are applied to each connection (left and right) as if the panel were rectangular for the corresponding beam depth. The comparison is established in terms of the moment at the connection versus the average shear deformation of the panel that has been measured using the following relation:

$$\text{Average rotation of the panel} = (\text{inclin}(3) + \text{inclin}(4)) / 2 - \text{inclin}(5)$$

Inclinometer 3 and 4 measure the total rotation at the top and bottom part on the panel along the centre line (see Figure 3), and the reading of inclinometer 5 is subtracted to take into account the flexural rotation of the column at the joint level.

Figures 11a and 11b show the moment rotations curves corresponding to the tests E1A and E2A, respectively. The tests only provide the initial stiffness since they are only loaded in the linear elastic range, and the plot is hidden underneath the finite element one. Figures 12a and 12b show the moment rotations curves corresponding to the tests E1B and E2B, respectively. Table 3 compares the values of the stiffness obtained by the different methods, as well as the relative errors when compared to the experimental results.

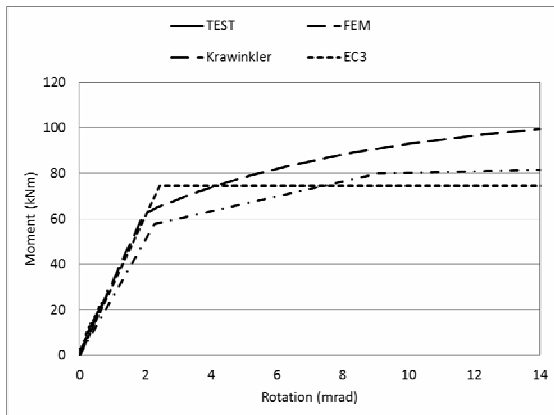


Figure 11a. Moment-rotation for test E1A

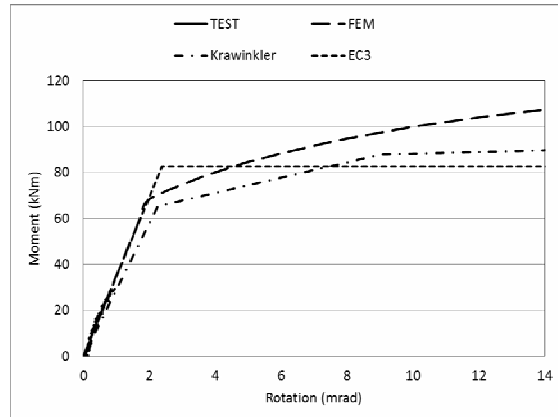


Figure 11b. Moment-rotation for test E2A

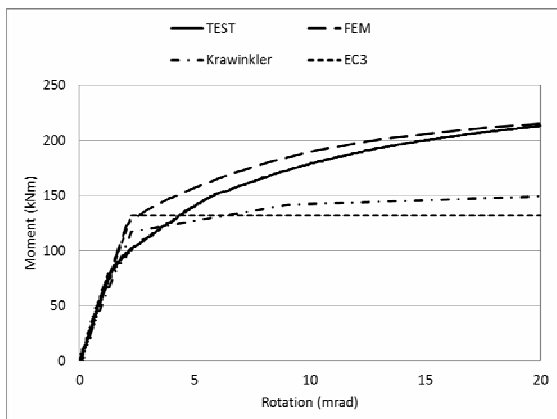


Figure 12a. Moment-rotation for test E1B

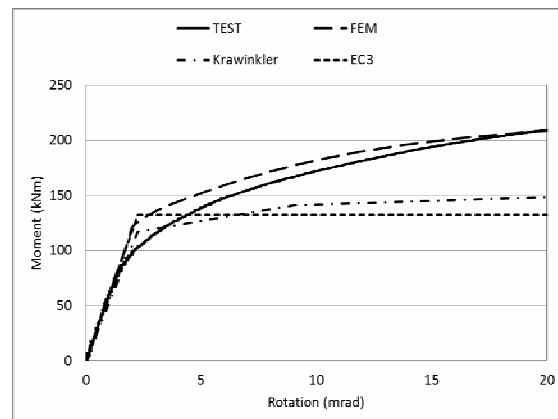


Figure 12b. Moment-rotation for test E2B

Table 3. Comparison of rotational stiffness (kNm/mrad).

	Test	FEM	Error (%)	EC3	Error (%)	EC3 with V_c	Error (%)	Krawinkler	Error (%)	
	E1A	32.2	32.1	-0.6	30.6	-5.3	33.4	3.6	25.4	-21.2
	E1B	61.8	60.2	-2.6	58.4	-5.6	70.5	14.0	51.7	-16.4
	E2A	35.4	34.9	-1.2	34.5	-2.5	38.5	8.7	28.9	-18.3
	E2B	60.1	59.4	-1.2	58.4	-2.7	69.2	15.2	51.7	-13.9

It may be seen that the predictions of the finite element model in terms of stiffness and resistance are quite good. The differences at the knee level may be due to the uncertainty in the modelling of the welding material properties. Eurocode 3 provides a very good prediction of the stiffness but a poor prediction of the resistance, even when including the additional resistance provided by the column flanges. Krawinkler's model underestimates both the stiffness and resistance, although the latter is better approximated than the Eurocode.

It is worth mentioning that the Eurocode does not account for the beneficial effect of the shear in the column, V_c . If that effect had been included, the stiffness values would have been those shown in Table 3 and the prediction would have been stiffer with higher errors.

4. CONCLUSIONS

In this paper we have investigated the shear performance of trapezoidal shear panels appearing in joints with unequal beam depths. Several tests have been performed as well as finite element simulations. The main conclusions can be summarized as follows:

1. The shear deformation zone corresponds to the upper rectangle when loading the shallow beam, and the whole trapezoid when loading the deep beam. Consequently the initial stiffness values of the left and right connections are different.
2. The finite element analysis predicts the stiffness with very good accuracy. Eurocode 3 approximates very well the initial stiffness of the left and right connections when using the dimensions of beam attached to the corresponding connection. Krawinkler's model tends to be less stiff because it considers a low shear area.
3. The total resistance of the connection are not well approximated by either the Eurocode or Krawinkler's model, although the latter provides a better approximation than the former. The finite element model predicts the resistance with sufficient accuracy.
4. More research is needed to better model the resistance and post-elastic behaviour of this type of joints.
5. The mechanisms of deformation at the left and right connections are different and this should be considered at the time of defining the joint stiffness for frame analyses.

ACKNOWLEDGMENT

The financial support provided by the Spanish Ministerio de Ciencia e Innovacion under contract grant BIA2010-20839-C01/C02 is gratefully acknowledged

REFERENCES

- Bayo, E., Cabrero, J.M., Gil, B. (2006). "An effective component based method to model semi-rigid connections for the global analysis of steel and composite structures". *Engineering Structures*, vol. 28 (pp. 97-108).
- Bayo, E., Gracia, J., Gil, B., Goñi, R. (2012). "An efficient cruciform element to model semirigid composite connections for frame analysis". *Journal of Constructional Steel Research*, vol. 72, (pp. 97–104).
- Curtis, H., Greiner, G. (1996). "A stress-based quadrilateral shear panel". *Finite element analysis and design*, vol. 21, (pp. 159-178).
- EN 1993-1-8-2005. European Committee for Standardization – CEN. Eurocode 3: Design of steel structures. Part 1.8: Design of joints, Brussels.
- Hashemi, B.H., Jazany, R.A. (2012). "Study of connection detailing on SMRF seismic behaviour for unequal beam depths". *Journal of Constructional Steel Research*, vol. 68 (pp. 150-164).
- Hoogenbroom, P., Blaauwendraad, J. (2000). "Quadrilateral shear panel". *Engineering Structures*, vol. 22 (pp. 1690-1698).
- Jordao, S. (2008) "Comportamento de juntas soldadas em nó interno com vigas de diferentes Alturas e aço de alta resistencia". PhD. Thesis. Departamento de Engenharia Civil. University of Coimbra. Portugal.
- Jordao, S., Simoes da Silva, L., Simoes, R. (2008) "Design rules proposal for high strength steel: internal nodes with beams of different heights". *Eurosteel 2008*. Graz, Austria.
- Krawinkler, H., Bertero, V., Popov, E. (1975). "Shear behaviour of steel frame joints". *Journal of the Structural Division*, vol. 101, (pp. 2317-2336).